



Acoustic Simulation of Multilayered Noise Control Treatment with Porous Material

Wenlong Yang ESI North America

Michael Dinsmore Acoustical Consulting Services

Alexis Castel and Ricardo O. de Alba Alvarez ESI North America

Roger Michna ConForm Automotive

Citation: Yang, W., Dinsmore, M., Castel, A., de Alba Alvarez, R.O., et al., "Acoustic Simulation of Multilayered Noise Control Treatment with Porous Material," SAE Technical Paper 2018-01-0144, 2018, doi:10.4271/2018-01-0144.

Abstract

Porous materials have been applied increasingly for absorbing noise energy and improving the acoustic performance. Different models have been proposed to predict the performance of these materials, and much progress has been achieved. However, most of the foregoing researches have been conducted on a single layer of porous material. In real application, porous materials are usually combined with other kinds of materials to compose a multilayered noise control treatment. This paper investigates the acoustic performance of such treatments with a combination of porous and non-porous media. Results from numerical

simulation are compared to experimental measurements. Transfer matrix method is adopted to simulate the insertion loss and absorption associated with three samples of a noise control treatment product, which has two porous layers bonded by an impervious screen. The elastic parameters of the solid phase of a foam or fiber mat are estimated by matching the simulated results to the tested data. It is concluded that appropriately considering the elasticity of the frame in the porous materials is the key to correctly simulate the acoustic performance of multilayer treatments, especially if the global stiffness of the treatment combined with its mass create a local resonance.

Introduction

In the past decades, porous materials have been applied increasingly in various fields for absorbing noise energy. Being porous means there are cavities, channels or interstices associated with the solid in the material. The sound waves can go through the porous materials but at the price of energy dissipation due to the thermal and viscous effect. To enhance the effectiveness, porous materials are usually employed with other kinds of materials, such as the barrier, in the form of multi-layer noise control treatment [2].

To investigate the acoustic performance of the porous materials has been a challenge to the engineering community. Each porous material has two phases, the solid frame and the fluid part. For representing the propagations of waves inside, different models have been proposed. The most classical one is the Biot's theory published in 1950s which derives the wave propagation from a stress-strain point of view based on a Lagrangian formulation [4, 5, 6]. Some simplified or modified models were also published since then. Basically, the models can be categorized according to the frame types: rigid, limp or elastic. Being rigid means there is only an acoustical wave propagating in the fluid phase, which is unable to generate the vibration in the solid phase and thus the frame is supposed motionless. The limp model can account for the inertia of the

frame in the modelling of their dynamic behavior, with the assumption that the stiffness of the frame is negligible. The elastic model, which increases the complexity, considers the elasticity of the frame and the energy exchange between structural energy and acoustic energy within the porous material. In elastic model, there are three types of waves and each wave type is present in both the frame and the fluid, which have properties predominately influenced by the frame properties. The full elastic porous model requires all the fluid properties and the elastic bulk properties [11].

Much progress has been achieved by the researchers in the past years for better understanding the acoustic performance of porous materials. Wang *et al.* [14] investigated the effect of compression on absorption by considering the elasticity of the frame. It concluded that the effect of the frame elasticity shall be considered if the resistivity of the porous material is large. Kidner and Hansen [9] reviewed the research on acoustic waves in porous media and compared the models used to predict the absorption characteristics of porous materials. It concluded that using the Biot model will result in a more complete description of the acoustics within the porous material. It also pointed out that empirical models could be applicable. Panneton [11] pointed out proper porous models is critical for the simulation of porous

material and suggested one to adopt the full poroelastic model when it is uncertain to determine the choice. However, the elasticity of the frame is a prerequisite for elastic model and the potential instabilities may come with the numerical simulation. Horoshenkov [8] suggested applying the acoustic models to estimate the morphological characteristics of the porous materials from the impedance tube test data.

Perhaps because of the complexity of the porous models, most of the above-mentioned researches were conducted on a single porous material, and especially on the absorption investigation. However, in industry applications, a porous material is seldom utilized alone. The porous materials are usually employed together with other kinds of materials, such as solid plate and impervious screen, to compose a multi-layer noise control treatment. Therefore, it is of high significance to conduct a thorough study on acoustic simulation of the multi-layer noise control treatment which contains porous materials.

The objective of this paper is to investigate the influence from the models of porous materials to the overall acoustic performance simulation of a multi-layer noise control treatment. Both acoustical test and numerical simulation are implemented for the research. Insertion loss and absorption measurements are fulfilled on three samples of a noise control treatment product. Each sample is with three layers, two porous layers and one screen layer. Both porous layers are made from the same fiber, while keeping one porous layer very light, limp and with high porosity and another one highly compressed and with high density. For acoustic simulation, the transfer matrix method is utilized, which employs transfer matrices to represent the wave propagation in different media. Different porous acoustical models are employed in the numerical simulation. For distinct porous models, the transfer and coupling matrices inside each material and among layers are different, and thus the difference could be detected. The measured values of the samples are employed to justify the simulation.

Theoretical Background

The Transfer Matrix Method (TMM) is employed to simulate the acoustic performance of the multilayers. In TMM, it is assumed that each layer is homogenous and isotropic and a matrix representation of sound propagation is used to model plane acoustic fields in stratified media. An internal transfer matrix and an interface transfer matrix are applied to represent the wave propagation inside each layer and between two adjacent layers, respectively. Based on these two kinds of transfer matrices, a global transfer matrix can be constructed to relate the acoustic parameters on both sides of the multilayers. TMM has been proven by multilayers with different natures: elastic solid, thin plate, septum, fluid and porous [1].

In this section, first reviewed are the elastic frame model, rigid frame model and limp frame model for porous. The transfer matrices associated with different porous models and the septum screen are then illustrated.

Porous Models

Elastic Frame Porous Model In Biot's theory, the acoustic performance of a porous material is modeled by simulating two compression waves and one shear wave propagating in the medium. The complex wave numbers of the two compression waves and the shear wave, δ_1 , δ_2 and δ_3 are

$$\delta_1^2 = \frac{\omega^2}{2(PR-Q^2)} \left[P\tilde{\rho}_{22} + R\tilde{\rho}_{11} - 2Q\tilde{\rho}_{12} - \sqrt{\Delta} \right] \quad (1)$$

$$\delta_2^2 = \frac{\omega^2}{2(PR-Q^2)} \left[P\tilde{\rho}_{22} + R\tilde{\rho}_{11} - 2Q\tilde{\rho}_{12} + \sqrt{\Delta} \right] \quad (2)$$

$$\delta_3^2 = \frac{\omega^2}{N} \left(\frac{\tilde{\rho}_{11}\tilde{\rho}_{22} - \tilde{\rho}_{12}^2}{\tilde{\rho}_{22}} \right) \quad (3)$$

where $\Delta = (P\tilde{\rho}_{22} + R\tilde{\rho}_{11} - 2Q\tilde{\rho}_{12})^2 - 4(PR-Q^2)(\tilde{\rho}_{11}\tilde{\rho}_{22} - \tilde{\rho}_{12}^2)$ and N is the shear modulus of the porous material. The frequency-dependent parameters $\tilde{\rho}_{11}$, $\tilde{\rho}_{12}$ and $\tilde{\rho}_{22}$ are the functions of frequency and the porous parameters like tortuosity (α_∞), air viscosity (η), viscous characteristic length (Λ), flow resistivity (σ) and porosity (ϕ). P , Q , R are the functions of parameters associated with both the frame phase and the fluid part, including the Bulk moduli of the frame and the fluid (K_b and K_f), the Poisson's ratio (ν), the shear modulus (N), the porosity (ϕ), the ratio of the specific heats (γ), the atmospheric pressure (P_0), the characteristic length (Λ'), the air viscosity (η), and the Prandtl number (B^2). Some of these parameters are further related to the elasticity of the frame. The equations for these parameters are somehow complicated and it will be tedious to list them in details. The interesting readers can refer to the classical book written by Allard and Atalla [1].

Rigid Frame Porous Model In the rigid model, the frame is supposed to be motionless, which means it has no displacement or deformation. This situation happens when the frame is constrained and rigid, heavy. It also occurs if the coupling effect between the fluid and solid is negligible, so that the solid frame will not vibrate by the excitation from the acoustic wave in the fluid phase. Consequently, there is only an acoustic compression wave in the porous material.

The following equivalent fluid wave model in the form of Helmholtz equation can represent the dynamical behavior of the rigid model

$$\Delta p + \frac{\tilde{\rho}_{eq}}{\tilde{K}_{eq}} \omega^2 p = 0 \quad (4)$$

where p is the fluid pore pressure; $\tilde{\rho}_{eq}$ is the effective density; and \tilde{K}_{eq} is the effective bulk modulus of the rigid frame equivalent fluid medium. The effective density and effective bulk modulus are complex valued and frequency dependent. In this paper, the Johnson-Lafarge model is adopted for calculating them [1, 10]. Using these effective properties, the wave number of the acoustic compression wave is given by $\omega \sqrt{\frac{\tilde{\rho}_{eq}}{\tilde{K}_{eq}}}$.

Limp Frame Porous Model The limp model assumes the frame of the porous material flexible and limp, and unable to resist to external excitations. Thus, there is no stress field associated with the frame, and there is only acoustic compression wave. This model is effective for cases such as that the solid particles suspend in a fluid medium or the porous material is with very low shear modulus. Similar to the rigid frame porous model, the following equivalent fluid equation can represent the dynamical behavior of limp frame porous model

$$\Delta p + \frac{\tilde{\rho}_{\text{limp}}}{\tilde{K}_{\text{eq}}} \omega^2 p = 0 \quad (5)$$

where $\tilde{\rho}_{\text{limp}}$ is an equivalent effective density accounting for the inertia of the frame and can be represented by

$$\tilde{\rho}_{\text{limp}} = \frac{\tilde{\rho} \tilde{\rho}_{\text{eq}}}{\tilde{\rho} + \tilde{\rho}_{\text{eq}} \tilde{\gamma}^2} \quad (6)$$

When comparing Eq. (4) and Eq. (5), one can easily find the only difference between the rigid model and limp model is whether the motion of the frame is considered. The performance of the two models mainly differs at the low frequency range. The limp model is usable when the elasticity of the frame is neglected, either due to the nature of the material or due to the mounting or excitation of the material.

Transfer Matrix Method

Transfer Matrix Method relies on transfer matrices to represent the sound propagation in layered media. In each layer, an internal transfer matrix can connect the acoustic parameters at one location to another. At the face connecting two adjacent layers, an interface matrix is employed to consider the continuity of stress and velocity. Combing the internal transfer matrices and the interface matrices, the global transfer matrix can be obtained, which relates the acoustic parameters on both sides of the multilayer system.

Each material relies on a specific model and several quantities to represent the acoustic field inside the material. The internal transfer matrices for different materials/models are distinct. Mathematically, sound propagation inside a layer is represented by a transfer matrix [T] such that

$$V(M) = [T]V(M') \quad (7)$$

where M and M' are two points set close to the forward and the backward face of the layer, respectively. The components of the vector $V(M)$ are the variables which describe the acoustic field at point M of the medium. The matrix [T] depends on the thickness h and the physical properties of each medium. For elastic porous material, six independent acoustic quantities could be chosen to predict the acoustical field: the two velocity components v_1^s and v_3^s of the frame, the velocity component v_3^f of the fluid, the two components σ_{33}^s and σ_{13}^s of the stress tensor of the frame, and σ_{33}^f in the fluid. Thus, the vector $V(M)$ is:

$$V(M) = [v_1^s(M), v_3^s(M), v_3^f(M), \sigma_{33}^s(M), \sigma_{13}^s(M), \sigma_{33}^f(M)]^T \quad (8)$$

The 6×6 transfer matrix [T] associated with elastic porous model is rather complicated. To fully display the matrix here will take pages. The interested readers can refer to Allard and Atalla [1].

Both rigid and limp porous models utilize the equivalent fluid equation to simulate its dynamical behavior. Thus, the acoustic field in a fluid medium is completely defined at point M by the vector

$$V^f(M) = [p(M), v_3^f(M)]^T \quad (9)$$

where p and v_3^f are the pressure and the x_3 component of the fluid velocity in the model, respectively. The 2×2 transfer matrix [T] is given by

$$[T] = \begin{bmatrix} \cos(k_3 h) & j \frac{k_3}{\omega \rho} \sin(k_3 h) \\ j \frac{k_3}{\omega \rho} \sin(k_3 h) & \cos(k_3 h) \end{bmatrix} \quad (10)$$

where h and ρ are the thickness and the density of the fluid medium, respectively. k_3 is the x_3 component of the wave number vector in the fluid, equal to $(k^2 - k^2 \sin^2 \theta)^{1/2}$ with k as the wave number and θ as the incidence angle. For

rigid and limp model, the wave number k is $\omega \sqrt{\frac{\tilde{\rho}_{\text{eq}}}{\tilde{K}_{\text{eq}}}}$ and $\omega \sqrt{\frac{\tilde{\rho}_{\text{limp}}}{\tilde{K}_{\text{eq}}}}$, respectively.

A septum screen can be simply modelled as a thin plate. In transfer matrix method, the following vector is utilized

$$V^s(M) = [v_1^s(M), v_3^s(M), \sigma_{33}^s(M), \sigma_{13}^s(M)]^T \quad (11)$$

where $v_1^s(M)$, $v_3^s(M)$, $\sigma_{33}^s(M)$ and $\sigma_{13}^s(M)$ are the x_1 and x_3 components of the velocity, the normal and tangential stresses at point M , respectively. The transfer matrix associated with the septum screen can be written as

$$[T] = \begin{bmatrix} 1 & 0 & 0 & 0 \\ 0 & 1 & 0 & 0 \\ 0 & -Z_s(\omega) & 1 & 0 \\ -Z'_s(\omega) & 0 & 0 & 1 \end{bmatrix} \quad (12)$$

where $Z_s(\omega) = j\omega m \left(1 - D \frac{\partial^4 v_3(M)}{m \omega^2 \partial x_1^4} \right)$ and $Z'_s(\omega) = j\omega m \left(1 - S \frac{\partial^2 v_1(M)}{m \omega^2 \partial x_1^2} \right)$ are the impedances. The quantities m , D , and S are the mass per unit area, the bending stiffness, and the membrane stiffness of the screen, respectively. For soft screen septum, the stiffness is usually negligible.

The interface matrices between two adjacent layers also depend on the specific models for representing the materials, which are detailed in Allard and Atalla [1].

Numerical Simulation

The study is based on three flat square samples of a noise control treatment product. The size of the samples is 1 m by 1 m. The total thicknesses of the samples are 20 mm, 25 mm and 30 mm, respectively. Each sample is with three layers, two porous layers bonded by one screen layer (the 20 mm thick sample is shown in Figure 1). Following the product specification, the two porous layers are named cap layer and loft layer, respectively, and they are made of the same fiber. The cap layer is highly compressed and with high density, while the loft layer is very light, limp and with high porosity. In all the three samples, the cap layer and the screen layer are unchanged. The only difference among the three samples is the loft layer, which is associated with the compression effect. The density, thickness and porous parameter of the two porous layers in three samples are listed in Table 1. The screen layer is with the thickness of 1 mil and area density of 30gsm.

The insertion loss and the absorption of the three samples were tested in an acoustic lab. During the measurement, the test samples were unbonded to the master structure. The reverberation chamber used for absorption measurements is approximately 10 cube meters in volume. It meets the requirements of SAE J2883 and is fully validated.

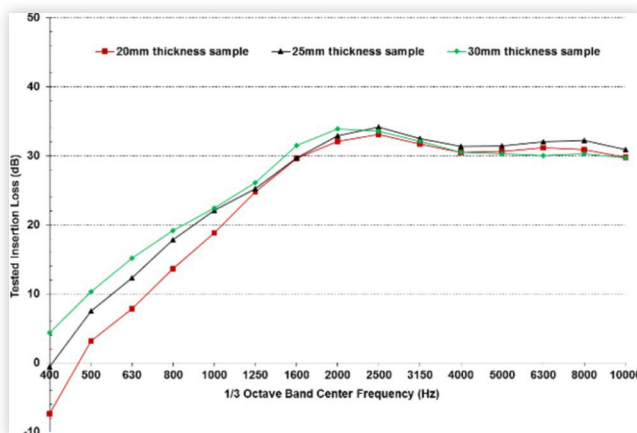
The tested curves of insertion loss and the absorption are shown in Figures 2 and 3, respectively. From Figure 2, it can

be observed that the energy leakage happened during the test, thus all the three tested insertion loss curves get flat after 4000 Hz. From Figure 2, one can also easily find there is resonance phenomenon with each sample. The reason is that the product is very nearly a double wall construction with the addition of a dense, absorptive fiber layer on top. A well-damped resonance occurs at 2000-2500 Hz due to the mass-spring effect of the relatively heavy cap (mass) layer vibrating on top of the spring represented by the trapped air below the film layer. Significant damping control is provided by viscous losses within the fiber layer below the film. The result is a light-weight construction in which the insertion loss rises at 10-12 dB at low frequencies and levels off to 30 dB or more at mid and high frequencies.

In this section, the acoustic simulation of the multilayered noise control product is conducted and the tested data is utilized to verify the simulation. Since the screen layer can be simulated omitting its stiffness, the most challenging part for the simulation is to choose appropriate models for the porous layers. In this study, the choice and setting of porous models are investigated by matching the simulation results to the tested values.

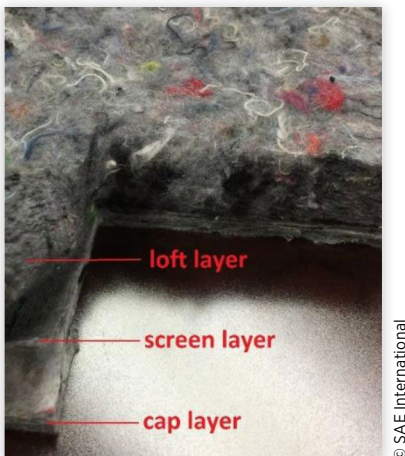
The classical transfer matrix method assumes a structure of infinite extent. To improve the simulation accuracy at low

FIGURE 2 Insertion loss measurement of the three samples



© SAE International

FIGURE 1 The 20 mm thickness sample



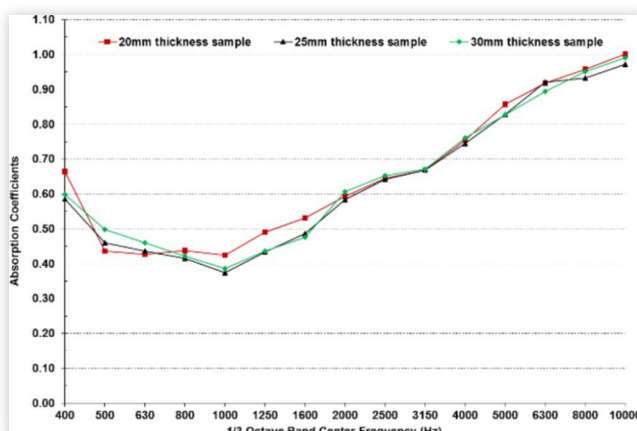
© SAE International

TABLE 1 Density, thickness and porous parameters of porous layers in the samples

Parameters	Cap layer	Loft layer		
		20mm sample	25mm sample	30mm sample
Thickness (mm)	6.4	13.6	18.6	23.6
Frame density (kg/m ³)	277	74	54	42
Porosity	0.81	0.95	0.96	0.97
Tortuosity	1.53	1.12	1.08	1.06
Viscous length (μm)	49	74	90	106
Thermal length (μm)	85	129	158	185
Resistivity (rayls/m)	117650	32046	20271	14466

© SAE International

FIGURE 3 Absorption coefficients measurement of the three samples



© SAE International

frequencies, the Finite Transfer Matrix Method [1], which replaces the radiation efficiency by the value of an equivalent baffled window, is employed in the simulation to account for the finite size effect.

Non-Elastic Models

When the elastic information of the layers is not available, one can take one of the following four assumptions: (a) simulating both porous layers by limp model; (b) simulating both porous layers by rigid model; (c) simulating the cap layer by rigid model and the loft layer by limp model; (d) simulating the cap layer by limp model and the loft layer by rigid model. The simulated insertion loss values for the 20 mm thick sample based on these four assumptions are shown in [Table 2](#). The simulated results from the four assumptions are very close, and all have a large deviation from the test data. The curves of tested insertion loss and simulation with assumption (d) are shown in [Figure 4](#). It is manifest that the simulation fails to display the resonance phenomenon, which is obviously shown in the tested curves. Clearly, all the non-elastic models are not suitable for the acoustic simulation of the samples in this study. To obtain the resonance phenomenon, the elastic contribution should be considered.

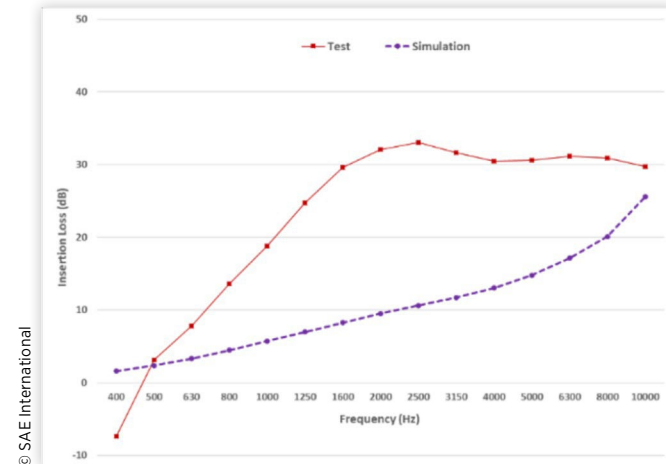
Elastic Models

As shown in [Table 1](#), the cap layer is highly compressed, while the loft layer is of low density and low resistivity. If applying elastic model to only one porous layer, the two straightforward assumptions could be: (1) simulating the cap layer by rigid model and loft layer by elastic model; (2) simulating the cap layer by elastic model and loft layer by limp model. In the elastic models, one need to specify the elastic properties, including Young's modulus, damping and Poisson's ratio.

TABLE 2 Insertion loss simulation results of 20 mm thickness sample from non-elastic porous models

Frequency (Hz)	Test (dB)	Both as rigid (dB)	Both as limp (dB)	Cap as limp; Loft as rigid (dB)	Cap as rigid; Loft as limp (dB)
400	-7.39	1.69	1.32	1.40	1.61
500	3.13	2.47	2.11	2.20	2.38
630	7.78	3.42	3.09	3.18	3.33
800	13.62	4.59	4.29	4.39	4.49
1000	18.80	5.84	5.58	5.68	5.74
1250	24.72	7.09	6.87	6.96	6.99
1600	29.60	8.37	8.18	8.28	8.28
2000	32.08	9.61	9.44	9.54	9.52
2500	33.05	10.70	10.56	10.64	10.62
3150	31.67	11.81	11.68	11.76	11.73
4000	30.45	13.14	13.01	13.10	13.05
5000	30.60	14.87	14.75	14.83	14.79
6300	31.14	17.20	17.09	17.16	17.13
8000	30.90	20.18	20.07	20.13	20.11
10000	29.75	25.64	25.52	25.59	25.57

FIGURE 4 Insertion loss of 20 mm thickness sample: Test vs. non-elastic model simulation

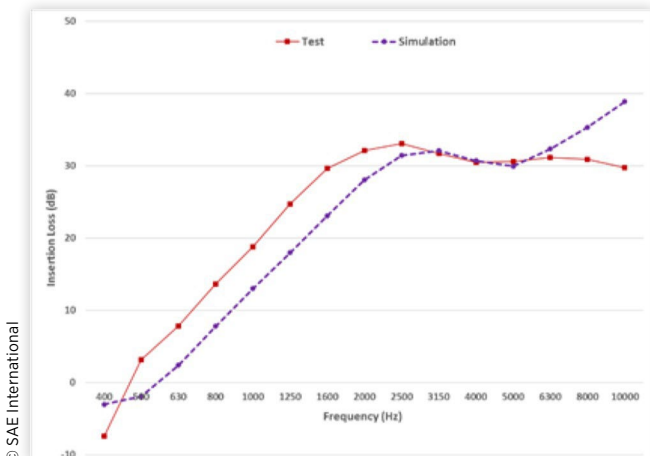


However, these parameters are not easy to measure for the porous material. In this study, these parameters are estimated, by fitting the simulation to the tested values.

Simulate the Cap Layer by Rigid Model and the Loft Layer by Elastic Model Based on this assumption, the different settings of Young's modulus, damping and Poisson's ratio for the loft layer are tried. It is found that the Young's modulus has the most significant influence to the simulation results, especially for capturing the resonance. While the damping and the Poisson's ratio only play a role around the resonance frequency. These two parameters will change the shape and slope of the curve in that frequency range. The best simulation result for the 20 mm thick sample is shown in [Figure 5](#), with the Young's modulus around 1.3 MPa, damping around 0.6, and Poisson's ratio around 0.2. Based on the simulation result of this sample, it seems choosing the rigid model for the cap layer and the elastic model for the loft layer is acceptable.

However, applying the same assumption to another two samples demonstrates that this assumption is wrong. The best

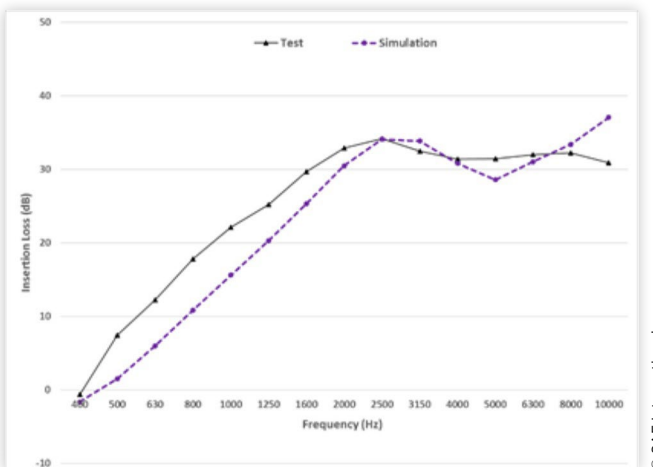
FIGURE 5 Insertion loss of 20 mm thickness sample: Test vs. simulating the loft layer as elastic



simulation results for the 25 mm thickness and 30 mm thickness samples are shown in [Figures 6](#) and [7](#), respectively. The simulation result in [Figure 6](#) is with Young's modulus around 2 MPa, damping around 0.4 and Poisson's ratio around 0.2. For [Figure 7](#), the corresponding elastic parameters are 2.2 MPa, 0.5 and 0.25. Obviously, the estimated Young's moduli are not reasonable. It has been proven that, while the frames of the porous are made of the same material, the frame in the more compressed one should have higher Young's modulus [\[12, 13\]](#). Another issue is that, for each sample, there is an obvious offset between the test and the best simulation in the frequency range below 2500 Hz, which is hard to explain.

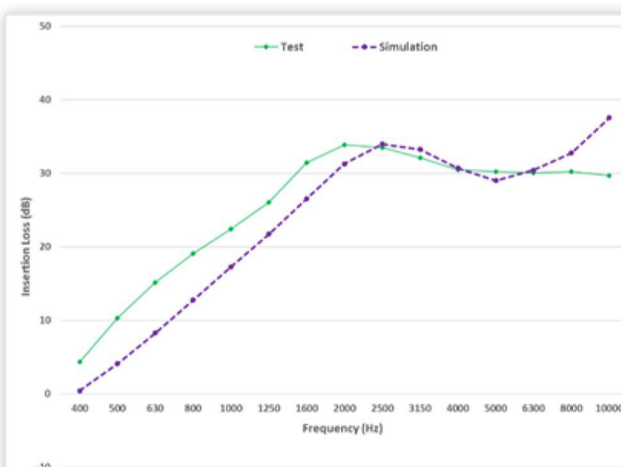
For the 20 mm-thick sample, with the estimated Young's modulus around 1.3 MPa, damping around 0.6, and Poisson's ratio around 0.2, the simulated absorption curve is shown in [Figure 8](#). The simulated curve is unable to match the tested curve, and they do not even show the same trend. The discrepancy demonstrates the deficiency of the assumption once again.

FIGURE 6 Insertion loss of 25 mm thickness sample: Test vs. simulating the loft layer as elastic



© SAE International

FIGURE 7 Insertion loss of 30 mm thickness sample: Test vs. simulating the loft layer as elastic

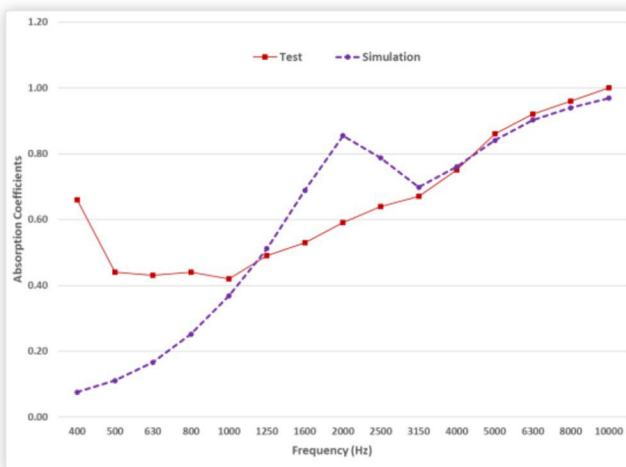


© SAE International

Simulate the Cap Layer by Elastic Model and the Loft Layer by Limp Model While simulating the cap layer by elastic model and the loft layer by limp model, the best simulations of insertion loss for the three samples are shown in [Figures 9](#) to [11](#). In all the figures, the tested and simulated insertion losses match each very well before the energy leakage happens in the test. The resonance phenomenon is successfully simulated and there is no similar offset as those shown in [Figures 5](#) to [7](#). For three samples, the estimated elastic frame parameters of the cap layer for simulating the best match are the same, with the Young's modulus around 0.55 MPa, damping around 0.5 and Poisson's ratio around 0.25. The consistency of the estimated elastic parameters can justify the assumption of the models.

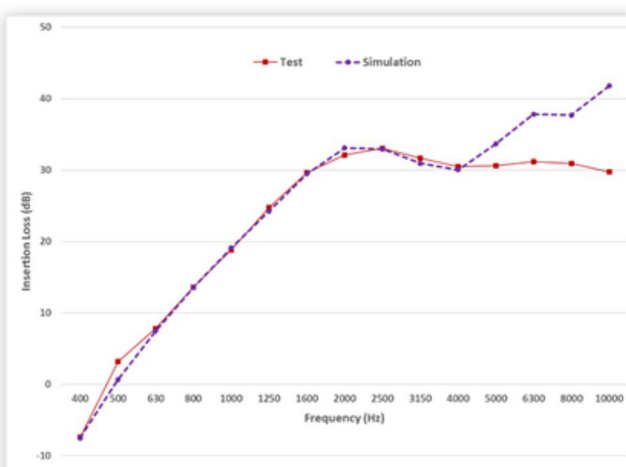
To further evaluate the assumption, the estimated elastic parameters of the cap layer (Young's modulus around 0.55 MPa, damping around 0.5 and Poisson's ratio around 0.25) are employed together with the limp assumption of the loft layer to simulate the absorption coefficients of the samples. The comparison of the estimated and tested absorption

FIGURE 8 Absorption coefficients of 20 mm thickness sample: Test vs. simulating the loft layer as elastic



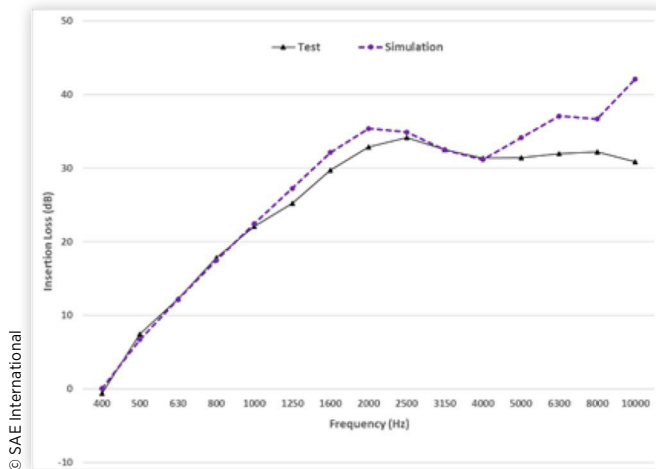
© SAE International

FIGURE 9 Insertion loss of 20 mm thickness sample: Test vs. simulating the cap layer as elastic



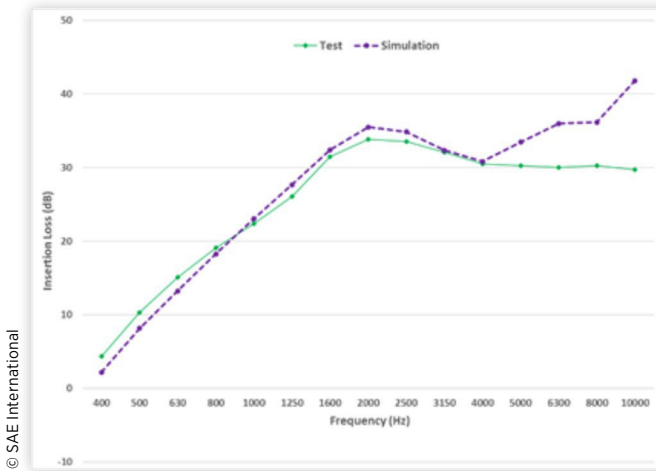
© SAE International

FIGURE 10 Insertion loss of 25 mm thickness sample: Test vs. simulating the cap layer as elastic



© SAE International

FIGURE 11 Insertion loss of 30 mm thickness sample: Test vs. simulating the cap layer as elastic

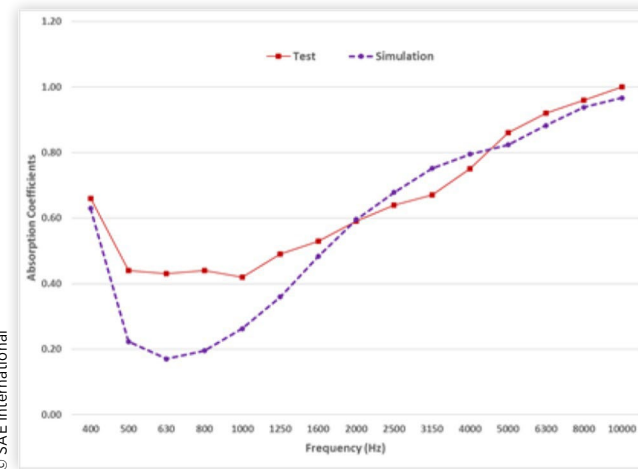


© SAE International

coefficients for the 20 mm, 25 mm and 30 mm samples are shown in Figures 12 to 14, respectively. The simulated and tested absorption curves have the similar trend and match very well. The match between the simulation and test are much better than what is shown in Figure 8, which demonstrates that attributing the elastic contribution to which layer is of high significance to the overall performance of multi-layered noise control treatment. One may notice there is some difference between the simulation and test at the low frequency range. This may come from the test deficiency or the inaccuracy of the porous parameters in Table 1.

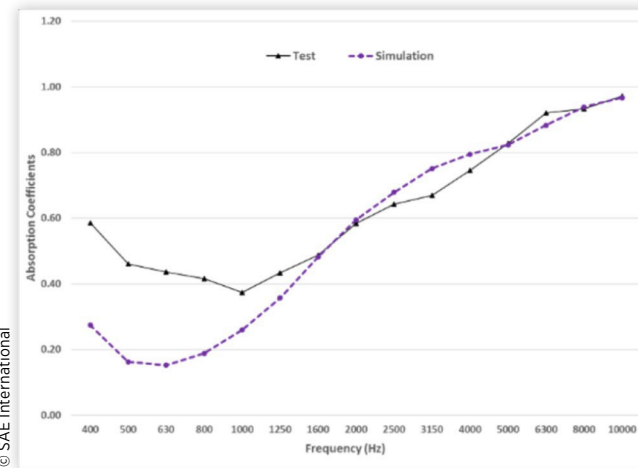
It must be pointed out that, simulating both porous layers by elastic models may generate even better simulation results. However, this will involve more unknown parameters and increase the complexity of the research. It is also difficult to verify the accuracy of the unknown elastic parameters, which need be estimated by just three samples. For the study in this research, simulating the cap layer by elastic model and the loft layer by limp model has been successfully justified. The accuracy is also acceptable from the viewpoint of engineering application.

FIGURE 12 Absorption coefficients of 20 mm thickness sample: Test vs. simulating the cap layer as elastic



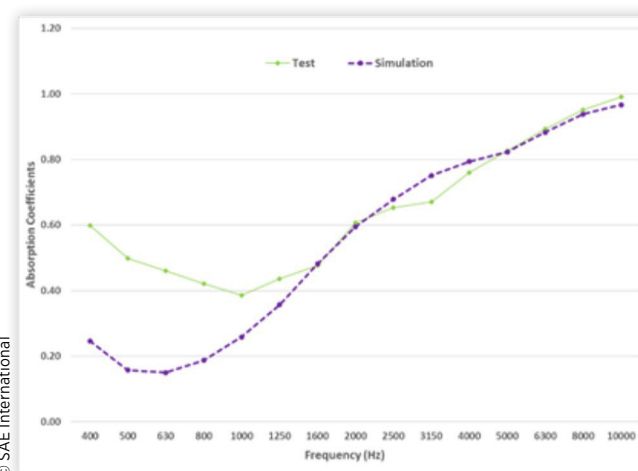
© SAE International

FIGURE 13 Absorption coefficients of 25 mm thickness sample: Test vs. simulating the cap layer as elastic



© SAE International

FIGURE 14 Absorption coefficients of 30 mm thickness sample: Test vs. simulating the cap layer as elastic



© SAE International

Conclusion

In this paper, the acoustic performance associated with three samples of a noise control treatment product was simulated by transfer matrix method. The noise control treatment product has two porous layers bonded by an impervious screen. In the simulation, different porous models were tried and investigated. For elastic porous model, the elastic parameters of the frame were estimated by matching the simulated insertion loss to the tested data.

From the research, it is concluded that adopting which model to represent the sound propagation in the porous material is crucial for its acoustic simulation. To consider the elasticity of the frame in the porous materials is the key to correctly simulate the insertion loss and absorption of the product. Without the elastic contribution, the simulation was unable to match the test data or even capture the trend.

Another conclusion is, for the acoustic simulation on noise control treatment with multiple porous layers, attributing the elastic contribution to which layer should be carefully investigated. If the study of this paper was based just on the insertion loss of the 20 mm thick sample, simulating the loft layer by elastic model and cap layer by rigid model can mislead one to accept a wrong model assumption. The reasonable model for the noise control treatment product was successfully obtained after comparing the acoustic simulation on three different samples.

References

1. Allard, J.F. and Atalla, N., "Propagation of Sound in Porous Media: Modelling Sound Absorbing Materials," (Chichester, John Wiley & Sons, 2009).
2. Arenas, J.P. and Crocker, M.J., "Recent Trends in Porous Sound-Absorbing Materials," *Sound & Vibration* 44:12-17, 2010.
3. Attenborough, K., "Acoustical Characteristics of Porous Materials," *Physics Reports (Review Section of Physics Letters)* 82(3):179-227, 1982.

4. Biot, M.A., "General Solutions of the Equations of Elasticity and Consolidation for a Porous Material," *Journal of Applied Mechanics* 78:91-96, March 1958.
5. Biot, M.A., "Theory of Propagation of Elastic Waves in a Fluid-Saturated Porous Solid. I. Low-Frequency Range," *The Journal of the Acoustical Society of America* 28:168-178, 1956.
6. Biot, M.A., "Theory of Propagation of Elastic Waves in a Fluid-Saturated Porous Solid. II. Higher Frequency Range," *The Journal of the Acoustical Society of America* 28:179-191, 1956.
7. Castagnede, B., Aknine, A., Brouard, B., and Tarnow, V., "Effects of Compression on the Sound Absorption of Fibrous Materials," *Applied Acoustics* 61:173-182, 2000.
8. Horoshenkov, K.V., "Porous Material Characterization via Acoustical Methods," The 22nd International Congress of Sound and Vibration, Florence, Italy, July 2015.
9. Kidner, M.R.F. and Hansen, C.H., "A Comparison and Review of Theories of the Acoustics of Porous Materials," *International Journal of Acoustics and Vibrations* 13(3), September 2008.
10. Lafarge, D., Lemarinier, P., Allard, J.F., and Tarnow, V., "Dynamic Compressibility of Air in Porous Structures at Audible Frequencies," *The Journal of the Acoustical Society of America* 102(4):1995-2006, 1997.
11. Panneton, R.E., "Comments on the Limp Frame Equivalent Fluid Model for Porous Media," *Journal of Acoustical Society of America* 122(6):EL217-EL222, 2007.
12. Pritz, T., "Dynamic Young's Modulus and Loss Factor of Plastic Foams for Impact Sound Isolation," *Journal of Sound and Vibration* 178(3):315-322, 1994.
13. Wang, J.C., "Young's Modulus of Porous Materials," *Journal of Materials Science* 19:801-808, 1984.
14. Wang, C.-N., Kuo, Y.-M., and Chen, S.-K., "Effects of Compression on the Sound Absorption of Porous Materials with an Elastic Frame," *Applied Acoustics* 69:31-39, 2008.

Contact Information

Wenlong Yang

ESI North America

32605 W12 Mile Road, Suite 350, Farmington Hills, MI 48334, USA
wenlong.yang@esi-group.com